

SCIENTIFIC REPORTS



OPEN

N-tert-butylmethanimine *N*-oxide is an efficient spin-trapping probe for EPR analysis of glutathione thiyl radical

Received: 06 September 2016

Accepted: 10 November 2016

Published: 12 December 2016

Melanie J. Scott¹, Timothy R. Billiar¹ & Detcho A. Stoyanovsky²

The electron spin resonance (EPR) spin-trapping technique allows detection of radical species with nanosecond half-lives. This technique is based on the high rates of addition of radicals to nitrones or nitroso compounds (spin traps; STs). The paramagnetic nitroxides (spin-adducts) formed as a result of reactions between STs and radical species are relatively stable compounds whose EPR spectra represent “structural fingerprints” of the parent radical species. Herein we report a novel protocol for the synthesis of *N*-tert-butylmethanimine *N*-oxide (EBN), which is the simplest nitrone containing an α -H and a tertiary α' -C atom. We present EPR spin-trapping proof that: (i) EBN is an efficient probe for the analysis of glutathione thiyl radical (GS^\bullet); (ii) β -cyclodextrins increase the kinetic stability of the spin-adduct EBN/*SG; and (iii) in aqueous solutions, EBN does not react with superoxide anion radical ($O_2^{\bullet-}$) to form EBN/*OOH to any significant extent. The data presented complement previous studies within the context of synthetic accessibility to EBN and efficient spin-trapping analysis of GS^\bullet .

The electron spin resonance (EPR) spin-trapping technique is an analytical method that allows detection of radical species with nanosecond half-lives. This technique is based on the high rates of addition of radicals (X^\bullet) to nitrones (Fig. 1, **1**) or nitroso compounds (spin traps; STs)^{1–3}. The paramagnetic nitroxides (spin-adducts; **2**) formed as a result of reactions between STs and radical species are relatively stable compounds ($t_{1/2}$ (spin-adducts) = seconds – hours) whose EPR spectra represent “structural fingerprints” of the parent radical species. To date, over 100 nitrones have been assessed as STs^{4,5} and the NIH spin-trapping database contains more than 10,000 entries from experiments performed with approximately 20 STs (<http://tools.niehs.nih.gov/stdb/>).

Analysis of EPR spectra and the stability of analogous series of spin-adducts indicates that cyclic STs with an α -H and a tertiary α' -C atom (Fig. 1, denoted in red and blue color, respectively) tend to form nitroxides with more resolved EPR spectra than their acyclic analogues⁴ and that hindrance of the nitroxide group stabilizes^{6–8} spin-adducts while polarization of the N-C α bond destabilizes them^{9,10}. The sensitivity of the spin-trapping technique is negatively affected by the dismutation of α -H spin-adducts to nitrones and hydroxylamines^{8,11}, whereas analyses in biological matrices are further complicated by the propensity of nitroxides to undergo one-electron reduction or oxidation either to “EPR-silent” hydroxylamines or to oxoammonium salts^{12–14}. The short half-lives of most spin-adducts necessitate the performance of analyses under steady-state conditions in which radical species are generated at considerable rates. Hence, there is a continuous effort to enhance the sensitivity of the EPR spin-trapping technique via identification of nitrones that form spin-adducts with increased stability.

In this paper, we report the spin-trapping analysis of selected biologically-relevant radical species by *N*-tert-butyl(methylideneamine) *N*-oxide (EBN; Fig. 1). We provide experimental proof that EBN reacts with glutathione thiyl radical (GS^\bullet) to form EBN/*SG, which exhibits a distinct EPR Spectrum. We further show that EBN/*SG is a relatively stable nitroxide as compared to spin-adducts of GS^\bullet with a number of widely used STs, and that β - and β -methyl-cyclodextrin (β -CD and β -Me-CD) extend the analytical window for assessment of GS^\bullet by increasing the kinetic stability of EBN/*SG.

¹Department of Surgery, University of Pittsburgh, Pittsburgh, Pennsylvania, USA. ²Department of Environmental and Occupational Health, University of Pittsburgh, Pittsburgh, Pennsylvania, USA. Correspondence and requests for materials should be addressed to D.A.S. (email: dstoyanovsky@gmail.com)

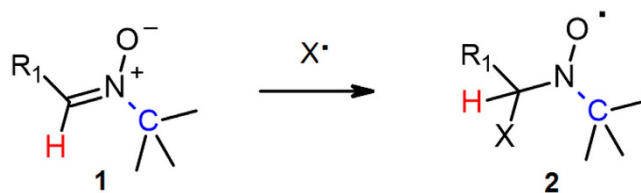


Figure 1. Nitrones react with radicals to form nitroxides.

Results and Discussion

Synthesis of EBN. EBN, the simplest nitron containing an α -H and a tertiary α' -C atom, has been extensively used as a reagent for cycloaddition reactions^{15–17}. In early spin-trapping studies with nitroso compounds, Chalfont *et al.* noted that EBN can be used as an alternative ST for detection of carbon-centered radicals^{18,19}. However, EPR spin-trapping data obtained with this nitron have not been reported thus far.

Coupling either of 2-methyl-2-nitroso-propane with diazomethane²⁰ (CAUTION, highly toxic compound) or of aqueous formaldehyde with *N-tert*-butylhydroxylamine (BHA)²¹ affords EBN in good to excellent yields. Following the latter protocol, we attained vacuum distillation of EBN, but failed to obtain a nitron fraction that was free of trace amounts of nitroxides, which ultimately interfere with EPR spin-trapping experiments. Purification of the nitron by activated charcoal or by column chromatography also proved difficult as the end reaction products exhibited comparable polarity. Hence, we optimized the synthetic protocol via assessment of the effects of solvents and the source of formaldehyde on the yield of EBN. EPR-grade EBN was obtained in quantitative yield via treatment of BHA hydrochloride with an excess of paraformaldehyde in CH_2Cl_2 , as described in Methods.

Spin-trapping of GS^\bullet by EBN. The metabolism of redox-sensitive xenobiotics often proceeds with generation of free radicals, which, in turn, react with thiols to form thiyl radicals. As glutathione is the most abundant cellular thiol, its oxidation by free radicals to GS^\bullet is a preponderant reaction, and the formation of GS^\bullet is viewed as a toxicological event as this radical species abstracts H atoms from cellular molecules, reacts with sulfhydryls to form disulfides, and adds to double bonds^{22,23}.

The detection of GS^\bullet in biological matrices is difficult because its half-life is in the nano-to micro-second scale²⁴. Research in the 1980s demonstrated that GS^\bullet reacts with 5,5-dimethyl-1-pyrroline *N*-oxide (DMPO) to form DMPO/ $\bullet\text{SG}$ (Fig. 2), which exhibits a specific four-line EPR spectrum^{25–28}. While this protocol proved instrumental in the elucidation of fundamental redox reactions of GSH, its application is limited by the low stability of DMPO/ $\bullet\text{SG}$ ($t_{1/2} \approx 50$ s)^{28–31}. Recent analyses of the kinetics of formation and decay of a number of GS^\bullet -derived spin-adducts have identified 5-(diethoxyphosphoryl)-5-methyl-1-pyrroline-*N*-oxide (DEPMPO) and *trans*-Mito-DEPMPO as STs that form kinetically more stable spin-adducts with GS^\bullet than DMPO (Fig. 1)³². To extend the structure-activity relationship study of the spin-trapping analysis of GS^\bullet , we have carried out experiments with EBN, which is a common structural motif of a number of widely-used STs (Fig. 2; common bonds in nitrones are denoted in red).

The data presented in Fig. 3A show the spin-trapping of GS^\bullet with EBN. We generated GS^\bullet via photolytic homolysis of the S-N bond of *S*-nitrosoglutathione (GSNO)³⁰. At ambient luminance (<400 lux), the reaction system consisting of GSNO and EBN did not exhibit any EPR activity (Fig. 3A1, black trace). Irradiation of the solution with visible light (515 nm cutoff filter; 1×10^5 Lux) led to the appearance of a seven-line EPR spectrum with hyperfine splitting constants (in mT) of $a_{\text{H}} = 0.729$ and $a_{\text{N}} = 1.607$, which was assigned to EBN/ $\bullet\text{SG}$ (Fig. 3A1, red tracings). In Fig. 3A2 is presented a computer simulation of the EPR spectrum of EBN/ $\bullet\text{SG}$. When GS^\bullet was spin-trapped by 50 mM EBN in the presence of 100 mM and 200 mM DMPO, the magnitude of the EPR spectrum of EBN/ $\bullet\text{SG}$ decreased by 33% and by 66%, respectively, indicating that $K_{\text{EBN}}^{\text{SG}} \approx 1.5 K_{\text{DMPO}}^{\text{SG}}$ (data not shown; comparison of the rate constants were made as reported in ref. 33; $K_{\text{DMPO}}^{\text{SG}} = 1 \times 10^8 \text{ M}^{-1} \text{ s}^{-1}$)¹⁰.

The reaction solution containing EBN and GSNO was illuminated until EBN/ $\bullet\text{SG}$ reached a steady-state concentration, after which interruption of the illumination led to a continuous decrease of the EPR spectrum with an apparent $t_{1/2}^{\text{(EBN/SG)}}$ of 120 s (Fig. 3A3, blue lines). No changes in either the formation or the decay of EBN/ $\bullet\text{SG}$ were observed in the pH interval of 5 to 8, nor in the presence of up to 1 M NaCl or LiClO_4 , indicating that these processes do not depend on ionic interactions (data not shown).

In Fig. 3B we present the EPR spectra of the spin-adducts of EBN with the thiyl radicals of L-cysteine, *N*-acetyl-D-penicillamine and 2-methyl-2-propanethiol, which were generated photolytically from the corresponding *S*-nitrosothiols (EBN/ $\bullet\text{SCys}$, EBN/ $\bullet\text{SNAP}$, and EBN/ $\bullet\text{SBu}$; blue lines, traces 1 ($a_{\text{H}} = 0.811$ and $a_{\text{N}} = 1.651$), 2 ($a_{\text{H}} = 0.884$ and $a_{\text{N}} = 1.722$) and 3 ($a_{\text{H}} = 0.897$ and $a_{\text{N}} = 1.762$), respectively). The spectra of EBN/ $\bullet\text{SG}$ (red traces, B1-3), EBN/ $\bullet\text{SNAP}$ and EBN/ $\bullet\text{SBu}$ were readily distinguishable (Fig. 3B2 and B3). The spectra of EBN/ $\bullet\text{SG}$ and EBN/ $\bullet\text{SCys}$ were similar but exhibited different intensity patterns (Fig. 3B1); for EBN/ $\bullet\text{SG}$, spectral maxima 3 and 5 were smaller than 4 and 6, whereas this ratio was reversed for EBN/ $\bullet\text{SCys}$. These data indicate that EBN can be used as a spin-trapping probe for identification of thiyl radicals with different substituents in C_α relative to the sulfur atom.

Stabilization of EBN/ $\bullet\text{SG}$ by cyclodextrins (CDs). The dismutation of α -H nitroxides to nitrones and hydroxylamines is a major reaction pathway leading to the decay of spin-adducts. The reaction proceeds via formation of a nitroxide-dimer wherein a single electron transfer from nitrogen to oxygen yields the ion pair

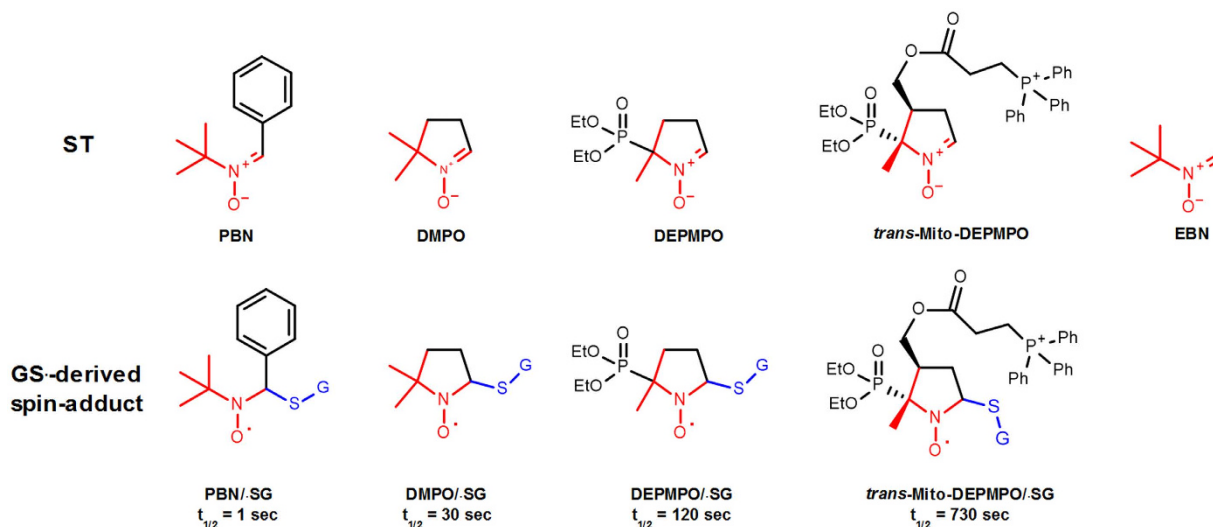


Figure 2. Structures of selected STs and their spin-adducts with GS^\bullet .

“hydroxylamine anion/oxoammonium cation”; tautomerization of the oxoammonium cation, with concomitant release of a proton, leads to the formation of a new nitron (Fig. 4; reviewed in ref. 34).

One strategy to increase the kinetic stability of spin-adducts containing α -H atoms is to impede their dimerization via inclusion into CDs. Cyclodextrins are cyclic polymers consisting of 6, 7 or 8 glucopyranoside units (α -CD, β -CD or γ -CD) which have the shape of toroids (7.9 Å), with the larger and smaller openings exposed to the solvent. They have hydrophilic interfaces and hydrophobic cavities with diameters of 4.7, 6, and 7.5 Å (α -, β - and γ -CD, respectively). CDs have a propensity for forming non-covalent inclusion complexes with a variety of hydrophobic organic molecules^{35,36}, including nitroxides^{37–40}. The spin-trapping of superoxide anion radical ($\text{O}_2^{\bullet-}$) with a series of STs in the presence of β -Me-CD has been shown to proceed with inclusion of the corresponding spin-adducts in the cavity of the cyclodextrin, thus increasing their half-lives^{41–46}.

The EPR spectra presented in Fig. 5 were obtained with generation of $\text{EBN}/\bullet\text{SG}$ in the presence of α -, β -, β -Me-, and γ -CD. In all experiments, EBN and CDs were used at 15 mM concentration (saturated solution of β -CD, 17 mM). As compared to the spectrum of $\text{EBN}/\bullet\text{SG}$, new EPR-active species were formed in the presence of β - and β -Me-, but not in the presence of α - and γ -CD. We observed the same spectral changes upon addition of CDs to pre-formed $\text{EBN}/\bullet\text{SG}$ (data not shown). Although marked spectral changes were detected in the hyperfine splitting constants of $\text{EBN}/\bullet\text{SG}$ upon its inclusion in CDs, resolved signals from the free and bound nitroxide were not obtained, and hence we did not assess the constants of the corresponding inclusion complexes. In the presence of β -CD, the EPR signal of $\text{EBN}/\bullet\text{SG}$ increased linearly with increases in the concentration of GSNO (0.005–0.2 mM). Since α - and γ -CD differ from β - and β -Me-CD only in the sizes of their cavities, spectral changes due to surface adsorption of the nitroxide on the outside of the cavities and/or spin-trapping of secondary radicals generated by reactions between GS^\bullet and/or $\text{EBN}/\bullet\text{SG}$ with CDs can be excluded. Furthermore, since β -CD has a hydrophobic channel with a diameter of 6 Å, inclusion of the whole $\text{EBN}/\bullet\text{SG}$ radical can be ruled out as well. The decrease in a_N in the presence of β -CDs indicates that the nitroxide function was compartmentalized in a more hydrophobic milieu, suggesting that the *tert*-butyl side of the spin-adduct was included in the CDs, whereas the hydrophilic, glutathionyl part of the molecule remained exposed to the bulk water.

In Fig. 6A, we show comparative kinetics of the decays of $\text{EBN}/\bullet\text{SG}$, $\text{DMPO}/\bullet\text{SG}$, and $\text{DEPMPO}/\bullet\text{SG}$. The apparent $t_{1/2}$ values of 50 and 120 seconds for $\text{DMPO}/\bullet\text{SG}$ and $\text{DEPMPO}/\bullet\text{SG}$ were in good agreement with previous studies^{29,30,32}, and the decay of $\text{EBN}/\bullet\text{SG}$ and $\text{DEPMPO}/\bullet\text{SG}$ exhibited similar kinetic profiles. Next, we assessed the kinetics of decay of $\text{EBN}/\bullet\text{SG}$ in the presence of CDs (Fig. 6B); in the presence of β -CD, the apparent $t_{1/2}$ of $\text{EBN}/\bullet\text{SG}$ increased from 120 s to 450 s, and the spectrum of the spin-adduct was readily detectable 90 min after interruption of the photolytic generation of GS^\bullet . Although $\text{EBN}/\bullet\text{SG}$ formed inclusion complexes with both β - and β -Me-CD, the stability of the spin-adduct in the presence of β -Me-CD was lower ($t_{1/2} = 190$ s). This suggests that either the rate of release of $\text{EBN}/\bullet\text{SG}$ from its complex with β -Me-CD was higher than from β -CD, presumably due to decreased hydrogen bonding between methylated OH groups and the nitroxide, or to the methyl groups obstructing its inclusion in the cyclodextrin.

Spin-trapping of $\text{O}_2^{\bullet-}$ and hydroxyl radical (HO^\bullet) by EBN. A considerable research effort has been directed toward the identification of STs that can be used for analysis of $\text{O}_2^{\bullet-}$ and HO^\bullet , which are radical species of considerable importance as reaction intermediates in various biological, radiolytic, and photochemical processes. In 1974, Harbour *et al.* reported that, in aqueous solutions, $\text{O}_2^{\bullet-}$ can be spin-trapped by DMPO⁴⁷. Although this method has been extensively used, it has considerable analytical limitations; the reaction of DMPO with $\text{O}_2^{\bullet-}$ is rather slow ($k^{\text{Superoxide}}_{\text{DMPO}} = 10 \text{ M}^{-1}\text{s}^{-1}$), $\text{DMPO}/\bullet\text{OOH}$ is an unstable spin adduct ($t_{1/2} = 50$ s), and the analysis is affected by trace amounts of transition metal ions and pH variations^{33,48}. In 1995, Frejaville *et al.* found that DEPMPO, an α -phosphorus-containing analogue of DMPO, reacts with $\text{O}_2^{\bullet-}$ to form $\text{DEPMPO}/\bullet\text{OOH}$, which is 15 times more stable than $\text{DMPO}/\bullet\text{OOH}$ ³³. Rosen *et al.* observed that increases in the

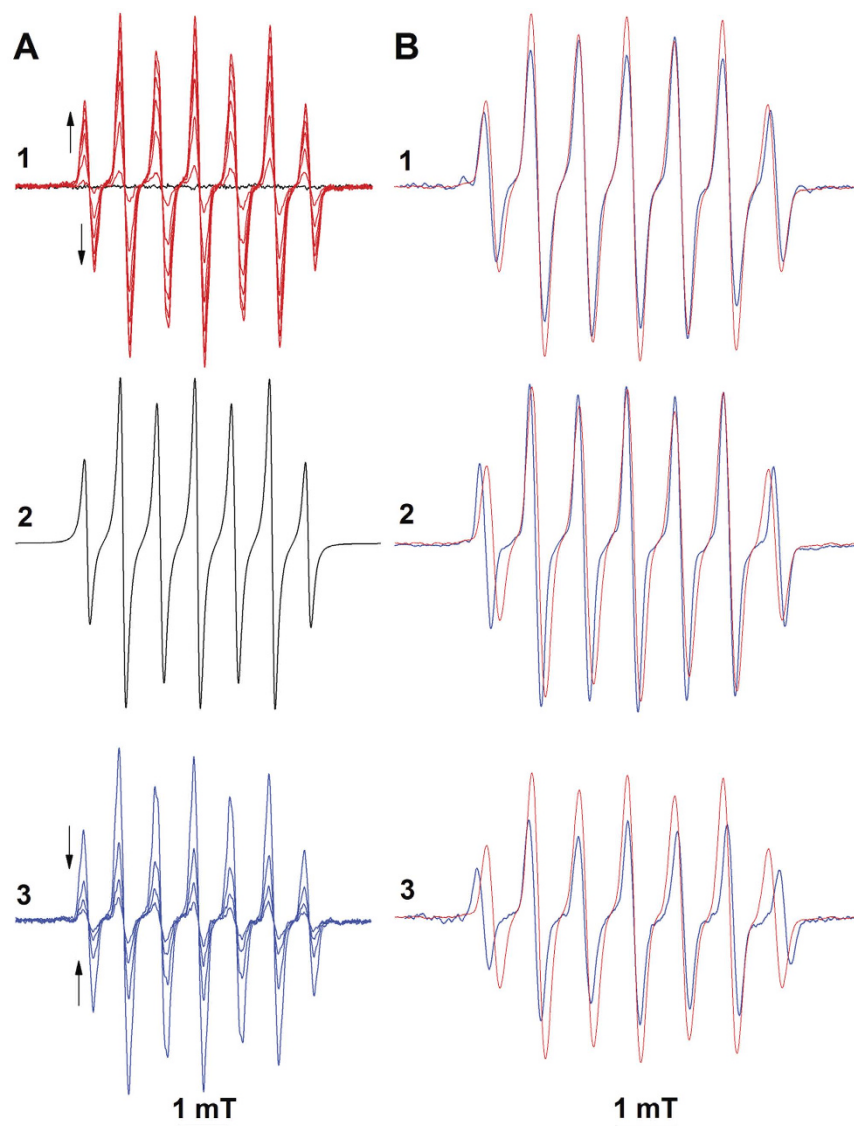


Figure 3. Spin-trapping of photolytically generated thiyl radicals by EBN. Reactions were carried out at 25 °C in 0.1 M phosphate buffer (pH 7.4) containing EBN (50 mM) and *S*-nitrosothiol (5 mM). **A1**- EPR spectra of GSNO and EBN prior to (light off; black trace) and after illumination (light on; red traces); **2**- computer simulation of the EPR spectrum of EBN/•SG; **3**- EPR-monitored decay of EBN/•SG (light off). Consecutive spectra were recorded with time intervals of 30 s (**1**) and 150 s (**3**). Arrows indicate the directions of the spectral changes. **B**- EPR spectra were recorded after illumination of *S*-nitrosothiols and EBN for 5 min; **1**- *S*-nitroso cysteine and EBN; **2** *S*-nitroso *N*-acetyl-D-penicillamine and EBN; *S*-nitroso 2-methyl-2-propanethiol and EBN. EPR spectra were recorded at an Amplification of 100.

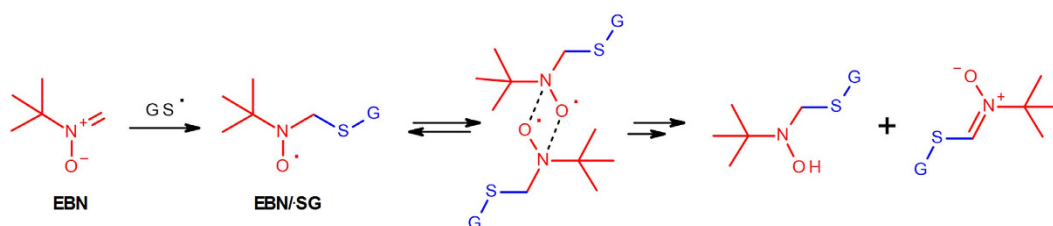


Figure 4. Nitroxides containing α -H atoms dismutate to nitrones and hydroxylamines.

bulkiness of alkyl substituents in third position of the pyrroline ring of DMPO leads to complete inhibition of the spin-trapping of $O_2^{-\bullet}$ ⁴⁹, as indicated by the formation of the corresponding nitroxides, while Allouch *et al.*

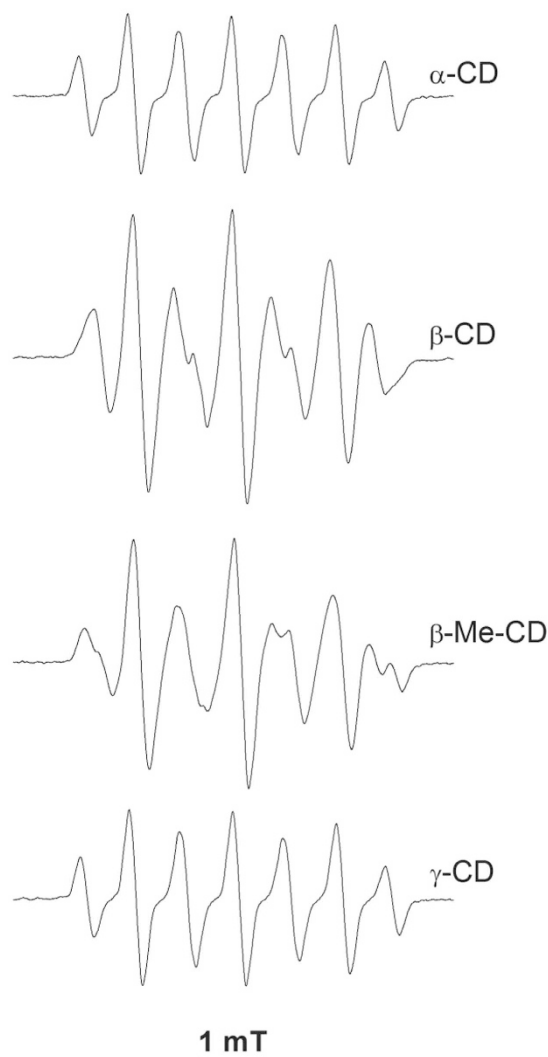


Figure 5. Effects of CDs on the EPR spectrum of EBN/•SG. EPR spectra (Amplification, 500) were recorded after photolytic homolysis of GSNO (5 mM) for 3 min in the presence of EBN (15 mM) and CDs (15 mM). All other incubation conditions are the same as indicated in the legend to Fig. 2.

found that introduction of electron-withdrawing groups in C α position of acyclic STs inhibits the spin-trapping of O $_2^{\bullet-}$ ⁵⁰. In a theoretical analysis of cyclic STs, Villamena *et al.* reported that the electronic density on the nitronyl C atom noticeably changes with introduction of substituents in C α - δ and thus affects the reactions of nitrones with O-centered radicals. However, these studies have not been extended to a structure-activity relationship that allows prediction of the spin-trapping affinity of nitrones for specific radical species.

Our attempts to obtain the spin-adduct of EBN with O $_2^{\bullet-}$ in aqueous solutions proved unsuccessful. In phosphate buffer (0.1 M; pH 7.4) containing catalase (300 U/mL) and EBN (50–200 mM), we did not observe the formation of EPR-active species upon addition of up to 0.4 mM KO $_2$ (Fig. 7A1; stock solution of KO $_2$ was prepared in DMSO containing an equimolar amount of 18-Crown 6). Similarly, we did not observe formation of EBN/•OOH when O $_2^{\bullet-}$ was enzymatically generated by the system hypoxanthine (HX; 0.5 mM)/xanthine oxidase (XO; 50 mU/mL; Fig. 7A2). Substitution of EBN with DEPMPO in the HX/XO system resulted in the appearance of the typical EPR spectrum of DEPMPO/•OOH (Fig. 7A3), thus indicating that O $_2^{\bullet-}$ was generated in the reaction solution. Superoxide dismutase (SOD; 30 U/mL) fully inhibited the formation of DEPMPO/•OOH (Fig. 7A4). In contrast to O $_2^{\bullet-}$, the generation of HO• in a Fenton-like system containing EBN led to the appearance of a well resolved nine-line EPR spectrum, which we assigned to EBN/•OH (Fig. 7B2; in mT, $a_H = 0.613$ and $a_N = 1.125$; H $_2$ O $_2$ + Fe $^{2+}$ → HO• + Fe $^{3+}$ + HO $^-$; EBN + HO• → EBN/•OH). No EPR activity was observed if any one of the reagents was omitted from the reaction system (Fig. 7B1). Introduction of DMSO in the reaction system led to the formation of EBN/•CH $_3$, which exhibited a distinct EPR spectrum (Fig. 7B3; CH $_3$ S(O)CH $_3$ + HO• → CH $_3^{\bullet}$ + CH $_3$ S(O)OH; EBN + CH $_3^{\bullet}$ → EBN/•CH $_3$). The identity of the latter nitroxide was confirmed by EPR analysis of authentic EBN/•CH $_3$, which was synthesized by methylation of EBN with CH $_3$ MgI (Fig. 7B4; in mT, $a_H = 1.199$ and $a_N = 1.854$).

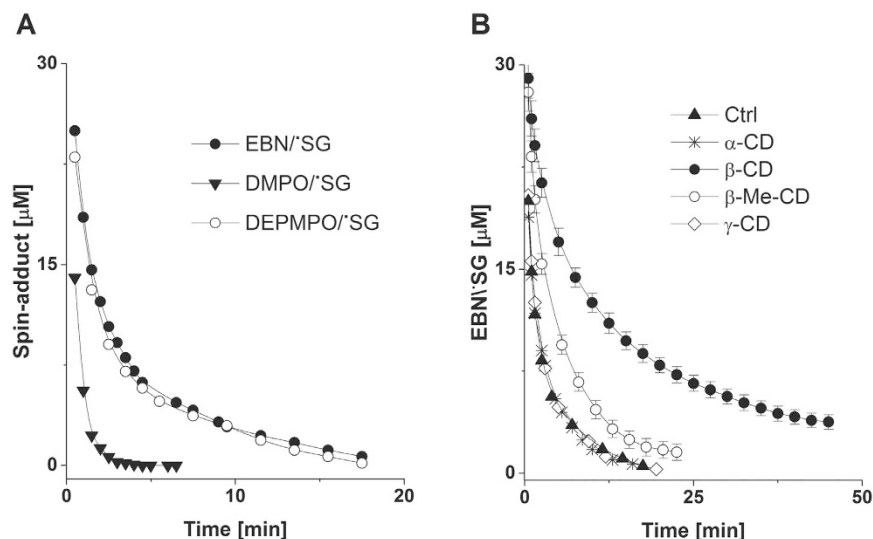


Figure 6. Effects of CDs on the decay of EBN/*SG. Photolytic homolysis of GSNO to GS[•] was carried out for 3 minutes in the presence of DMPO, DEPMPO and EBN. Thereafter, the light was switched off and decreases in the EPR spectra of spin-adducts were recorded over time in the absence (A) and the presence (B) of CDs (15 mM). Nitroxides were used at concentrations of 50 mM (A) and 15 mM (B). The spin concentration of nitroxides was determined by double integration of the EPR signals using 4-hydroxyl-1-TEMPO as a standard. All other reaction conditions are the same as indicated in the legend to Fig. 2. The data in panels B are presented as mean values of three independent experiments \pm the standard error.

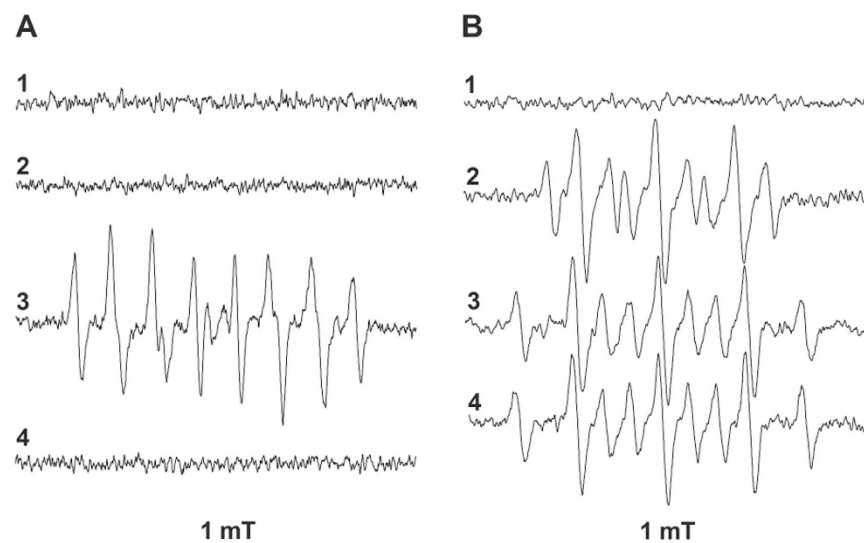


Figure 7. Spin-trapping of $O_2^{\bullet-}$, HO^{\bullet} and CH_3^{\bullet} by EBN. Reactions were carried out in 0.1 M phosphate buffer (pH 7.4) containing EDTA (0.05 mM). **A1-** EBN (50 mM), catalase (300 U/ml) and KO_2 (0.2 mM); **A2-** EBN, catalase, HX (0.5 mM) and XO (50 mU/mL); **A3-** DEPMPO (20 mM), catalase, HX and XO; **A4-** DEPMPO, catalase, HX, XO and SOD (30 U/mL). **B1-** H_2O_2 (0.05 mM) and EBN (20 mM); **B2-** plus $Fe(NH_4)_2SO_4$ (0.01 mM); **B3-** DMSO (0.2 M), EBN and H_2O_2 plus $Fe(NH_4)_2SO_4$; **B4-** authentic EBN/* CH_3 . EPR spectra were recorded at an Amplification of 1000.

We further carried out experiments to assess the reaction of EBN with $O_2^{\bullet-}$ in an aprotic solvent. Addition of a solution of 18-Crown 6/ KO_2 (final concentration, 0.4 mM) in anhydrous DMSO to DMSO containing EBN (20 mM) and H_2O (0.05 mM; Fig. 8A1) led to the appearance of a nine-line EPR spectrum, reflecting the formation of EBN/*OOH (Fig. 8A2; in mT, $a_H = 0.483$ and $a_N = 0.975$). The magnitude of the EPR signal decreased by 15% for 6 min, indicating that EBN/*OOH was unstable under these reaction conditions. An identical EPR spectrum was observed when a solution of EBN in DMSO was treated with H_2O_2 (20 mM) and Et_3N (100 mM), thus supporting the assignment of the EPR spectrum to EBN/*OOH; in the latter reaction system, a nucleophilic addition of HOO^- to the nitronyl C atom yielded EBN/OOH hydroxylamine, which autooxidized to EBN/*OOH nitroxide (data not shown). Dilution of a DMSO solution of EBN/*OOH with phosphate buffer (pH 7.4) resulted

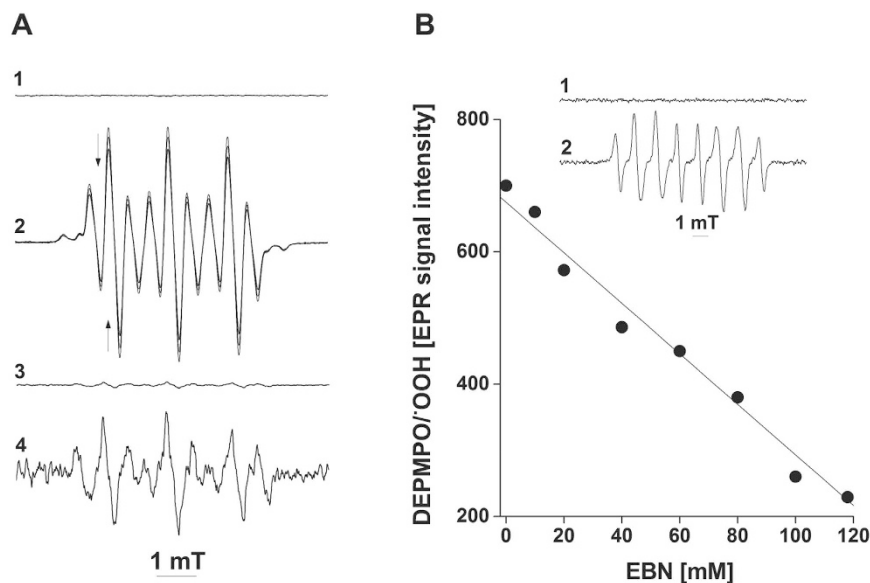


Figure 8. Spin-trapping of $O_2^{\bullet-}$ by EBN in DMSO and by DEPMPPO and EBN in aqueous solutions. A1- EBN (20 mM) in DMSO containing 0.05 mM H_2O ; A2- EBN, KO_2 (0.4 mM) and 18-Crown 6 (0.4 mM); $\Delta_{scan} = 2$ min; arrows indicate the direction of spectral changes); A3- EBN/ $^{\bullet}OOH$ (0.02 mL) plus phosphate buffer (pH 7.4; 0.08 mL; Amplification, 100); A4- the same spectrum as in A3 but recorded at an Amplification of 4000. B- Effects of EBN on the spin-trapping of $O_2^{\bullet-}$ by DEPMPPO. Reactions were carried out at 25°C in 0.1 M phosphate buffer (pH 7.4) containing catalase (300 units/mL). Inset, 1- DEPMPPO (10 mM); 2- DEPMPPO and 18-Crown 6/ KO_2 (0.1 mM). Spectra were recorded at an Amplification of 1000.

in the disappearance of the EPR spectrum of EBN/ $^{\bullet}OOH$ (Fig. 8A3) in less than 30 seconds, which is the approximate time required for sample preparation and data acquisition. However, we did observe the presence of trace amounts of a relatively stable nitroxide, less than 5% of the expected concentration of EBN/ $^{\bullet}OOH$, with hyperfine coupling constants suggesting the formation of EBN/ $^{\bullet}OH$ (Fig. 8A3 and 4- Amplification 100 and 4000, respectively).

In spin-trapping experiments, nitroxides are analyzed by EPR under steady-state conditions, where their rates of formation and decomposition define the analytical sensitivity of the corresponding protocol. While the data presented in Fig. 8A indicate that EBN/ $^{\bullet}OOH$ is an unstable compound in aqueous solutions, we were interested to assess the rate of the reaction of EBN and $O_2^{\bullet-}$ in phosphate buffer (pH 7.4). To this end, we carried out a competitive kinetics study of the reaction of DEPMPPO with $O_2^{\bullet-}$ in the presence of EBN, where the source of $O_2^{\bullet-}$ was 18-Crown 6/ KO_2 . Addition of $O_2^{\bullet-}$ (final concentration, 0.1 mM) to a solution of DEPMPPO (10 mM) in 0.1 M phosphate buffer (Fig. 8B; Inset, trace 1) resulted in the formation of DEPMPPO/ $^{\bullet}OOH$ (Fig. 8B; Inset, trace 2). The magnitude of the EPR signal of DEPMPPO/ $^{\bullet}OOH$ decreased linearly with increasing concentrations of EBN, with 50% inhibition of the formation of DEPMPPO/ $^{\bullet}OOH$ at ~100 mM EBN. These data indicate that the rate constant of the reaction of EBN with $O_2^{\bullet-}$ is one order of magnitude lower than that of DEPMPPO ($k_{superoxide}^{DEPMPPO} = 15 M^{-1}s^{-1}$)³³. Hence, in contrast to DMPO and its analogues, EBN is a suitable ST for analysis of $O_2^{\bullet-}$ formed in organic but not in aqueous solutions, where both the rate constant of its reaction with $O_2^{\bullet-}$ and the stability of EBN/ $^{\bullet}OOH$ are relatively low.

Spin-trapping of enzymatically-generated GS^{\bullet} with EBN. The low reactivity of EBN with $O_2^{\bullet-}$ in aqueous solutions suggests that this nitron can be used for spin-trapping analysis of secondary, $O_2^{\bullet-}$ -derived radicals in biological systems. This possibility is illustrated by the data presented in Fig. 9A. Generation of $O_2^{\bullet-}$ by HX/XO in the presence of EBN, GSH, and catalase resulted in the formation of EBN/ $^{\bullet}SG$; in neutral aqueous solutions, $O_2^{\bullet-}$ oxidized GSH to GS^{\bullet} with a rate constant⁵¹ of $10^3 M^{-1}s^{-1}$. Addition of SOD to the reaction system fully inhibited the formation of EBN/ $^{\bullet}SG$ (data not shown). In this system, the spin-trapping selectivity of EBN was reminiscent to the affinity of 2-H-imidazole-1-oxide for thiyl radicals but not for $O_2^{\bullet-}$ ⁵².

To further validate EBN as a spin-trapping probe for GS^{\bullet} , we assessed the formation of GS^{\bullet} in a reaction system consisting of myeloperoxidase from human leucocytes (MPx; 0.2 units/mL), phenol (0.01 mM), GSH (1 mM), and H_2O_2 (0.1 mM). In this system, phenol undergoes oxidation to phenoxyl radical, which is reduced back to phenol by GSH with concomitant generation of GS^{\bullet} ; in turn, GSH reacts with the latter to form a disulfide anion radical which transfers an electron to O_2 , yielding GSSG and $O_2^{\bullet-}$ ⁵³. In cells, this reaction sequence can occur without apparent consumption of phenol and GSH, whose concentration is maintained via reduction of GSSG by glutathione reductase (Fig. 10).

In the absence of EBN, the complete reaction system did not exhibit any EPR activity (Fig. 9B1), indicating that the concentration of radical species was below the detection limit of the EPR spectrometer. Addition of EBN led to the appearance of the EPR spectrum of EBN/ $^{\bullet}SG$, whose intensity increased until a steady-state

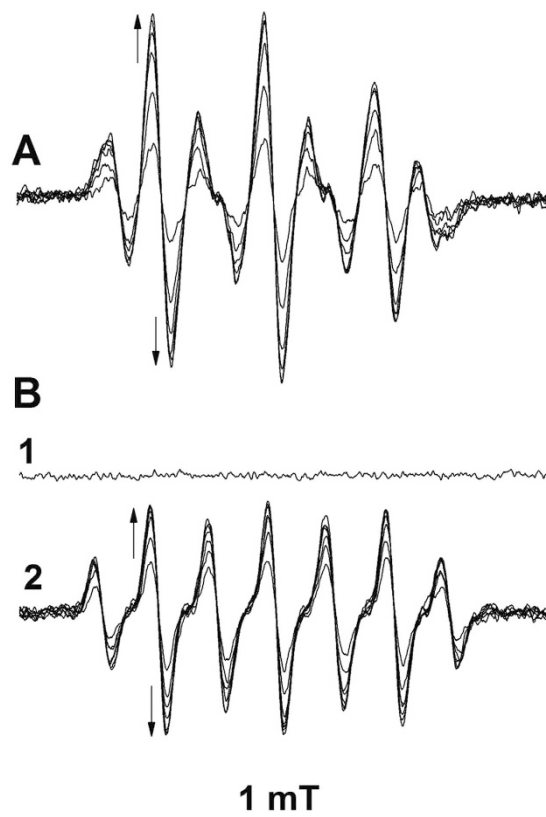


Figure 9. Spin-trapping of enzymatically-generated $O_2^{\cdot-}$. Reactions were carried out at 25 °C in 0.1 M phosphate buffer (pH 7.4). **A**- EBN (15 mM), β -CD (15 mM), GSH (2 mM), HX (0.5 mM), XO (50 mU/mL), and catalase (300 U/mL). **B1**- Phenol (0.01 mM), MPx (0.2 units/mL), H_2O_2 (0.1 mM), and GSH (1 mM); **B2**- Phenol, MPx, H_2O_2 , GSH and EBN (20 mM). Consecutive spectra were recorded with time interval of 120 s. Arrows indicate the directions of the spectral changes. EPR spectra were recorded at an Amplification of 1000.

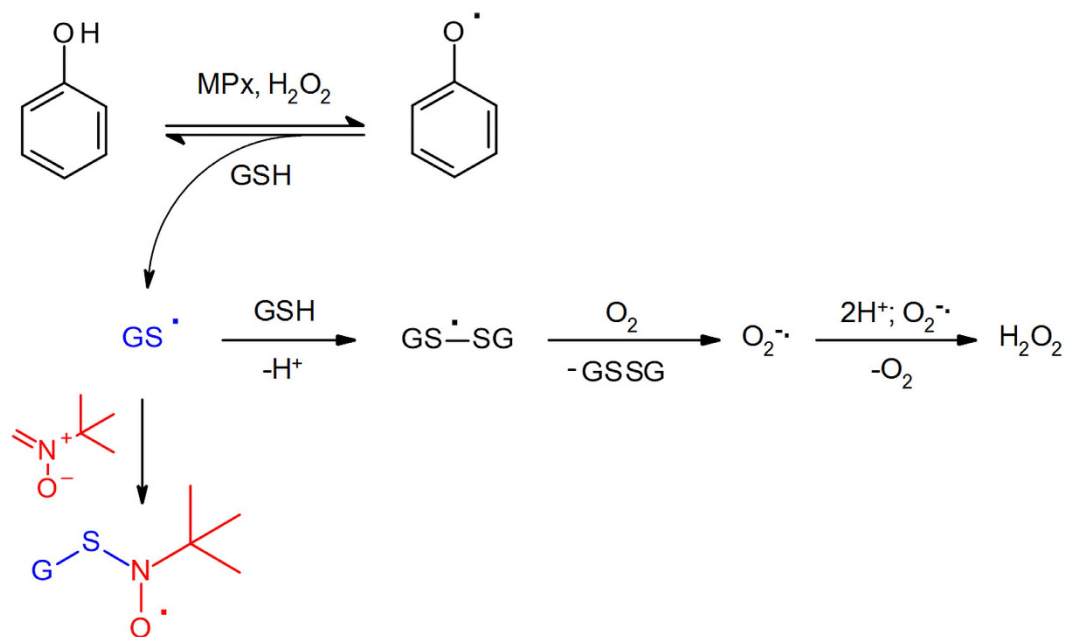


Figure 10. Phenol phenoxyl radical oxidizes GSH to GS^{\cdot} .

concentration of EBN/*SG has been reached. Elimination of H₂O₂ by addition of catalase to the reaction system led to disappearance of the EPR signal of EBN/*SG with a kinetic profile that was identical to that presented in Fig. 6A (data not shown).

Conclusions

The data presented herein complement previous studies within the context of synthetic accessibility to EBN and efficient spin-trapping analysis of GS•. From all nitrones tested thus far, *trans*-Mito-DEPMPO, DEPMPO and EBN form the most stable spin adducts with GS• ($t_{1/2}^{\text{trans-Mito-DEPMPO/SG}} = 730 \text{ sec}$; $t_{1/2}^{\text{DEPMPO/SG}} = 120 \text{ sec}$; and $t_{1/2}^{\text{EBN/SG}} = 120 \text{ sec}$). As compared to EBN, however, the synthesis of EPR grade DMPO analogues requires higher experimental effort. The relatively high rate of addition of GS• to EBN, the kinetic stability of EBN/*SG, and the well-resolved EPR spectrum of EBN/*SG define this nitron as an efficient molecular probe for GS•.

Materials and Methods

Reagents. All reagents used were purchased from Sigma-Aldrich Co. (St. Louis, MO). *N*-tert-butylhydroxylamine was synthesized as described in ref. 54. The solutions used in EPR-STs experiments were prepared in deionized and Chelex 100-treated water and in potassium phosphate buffer (pH 7.4). *S*-nitroso thiols were prepared by treatment of thiols with ethyl nitrite as reported in ref. 55. Methylation of EBN with CH₃MgI was carried out as reported in ref. 56.

Synthesis of *N*-tert-butylmethanimine oxide (EBN). Under an atmosphere of helium, a suspension of BHA hydrochloride (0.65 g; 5.2 mmol), paraformaldehyde (0.46 g; 15.3 mmol), anhydrous Na₂SO₄ (3.5 g; 24.6 mmol) and NaHCO₃ (2.5 g; 30 mmol) in 30 mL CH₂Cl₂ was stirred at 25 °C for 5 hours. Progression of the reaction was tracked via HPLC analysis of EBN. Chromatographic separations were carried out on a C18 matrix (column, Beckman; 4.6 × 250 mm; particle size, 5 μ) with methanol (40%) as the mobile phase (flow rate, 1 mL per min). Formation of EBN (retention time, 5.6 min; $\lambda_{\text{max}} = 230 \text{ nm}$; peak purity, 100%; software, EZchrom 4.3) was monitored with a SPD M10Avp Shimadzu diode array detector. Upon completion of the reaction, the suspension was filtered and the filtrate rotor-evaporated (30 °C; 250 torr), affording EBN as a colorless liquid (yield, 100%). MS *m/z*, calculated for C₅H₁₂NO (M)⁺ 102.09, found 101.88. Analogous yields of EBN were obtained with BHA acetate, which is a commercially available salt (Sigma-Aldrich, Co; St. Louis, MO). Following the protocol reported in reference 21, EPR-grade EBN was obtained via purification of the crude product by column chromatography (50 mg product on 150 g Silica Gel 60; mobile phase, 10% methanol in diethyl ether (v/v); yield, 45%).

Photolysis of *S*-nitrosothiols. Visible (white) light was provided by a Sylvania lamp type DWY (625 W) equipped with a spherical reflector. The light source was positioned 30 cm from the front of the EPR cavity, where Teflon tubing containing a solution of GSNO, EBN and DTPA (0.1 mM) in 0.1 M phosphate buffer (pH 7.4) was placed. The aperture of the cavity was equipped with a 515 nm cut-off filter (colored glass filter OG515; Melles Griot BV; Aalsbergen, Nederland). Light intensity was measured with a Datalogging Light Meter (Model 850008; SPER Scientific, LTD; Scottsdale, AZ).

EPR Spectroscopy. EPR spectra were recorded at room temperature using a JEOL-RE1X spectrometer (Kyoto, Japan). Spectrometer settings were: field center 335.094 mT, microwave power 10 mW, sweep time 30–120 s, time constant 0.1 s, and modulation width 0.2 mT. EPR spectra simulations were performed with a JEOL computer program.

References

- Iwamura, M. & Inamoto, N. Novel formation of nitroxide radicals by radical addition to nitrones. *Bull. Chem. Soc. Jpn.* **40**, 703–703 (1967).
- Janzen, E. G. & Blackburn, B. J. Detection and identification of short-lived free radicals by electron spin resonance trapping technique (spin trapping). Photolysis of organolead, -tin, and mercury compounds. *J. Am. Chem. Soc.* **91**, 4481–4490 (1969).
- Chalfont, G. R. & Perkins, M. J. A probe for homolytic reactions in solutions. II. The polymerization of styrene. *J. Am. Chem. Soc.* **90**, 7141–7142 (1968).
- Ouari, O., Hardy, M., Karoui, H. & Tordo, P. In *Electron Paramagnetic Resonance: Volume 22* Vol. 22, 1–40 (The Royal Society of Chemistry, 2011).
- Buettner, G. R. Spin trapping: ESR parameters of spin adducts. *Free Radic. Biol. Med.* **3**, 259–303 (1987).
- Amar, M. *et al.* Design concept for alpha-hydrogen-substituted nitroxides. *Nat. Commun.* **6**, 6070 (2015).
- Bowman, D. F. & Ingold, K. U. Kinetic application of electron paramagnetic resonance spectroscopy. III. Self-reactions of dialkyl nitroxide radicals. *J. Am. Chem. Soc.* **93**, 6555–6561 (1971).
- Toledo, H. *et al.* Synthesis and stability of cyclic alpha-hydrogen nitroxides. *Org. Biomol. Chem.* **13**, 10726–10733 (2015).
- Janzen, E. G., Kotake, Y. & Hinton, R. D. Stabilities of hydroxyl radical spin adducts of PBN-type spin traps. *Free Radic. Biol. Med.* **12**, 169–173 (1992).
- Polovyanenko, D., Plyusinin, V., Reznikov, V., Khrastov, V. & Bagryanskaya, E. Mechanistic study of the reactions of nitron spin trap PBN with glutathionyl radical. *J. Phys. Chem. B.* **112**, 4841–4847 (2008).
- Dupeyere, R. M. & Rassat, A. Nitroxides. XIX. Norpseudopelletierine-N-oxyl, a new, stable, unhindered free radical. *J. Am. Chem. Soc.* **88**, 3180–3181 (1966).
- Goldstein, S., Merenyi, G., Russo, A. & Samuni, A. The role of oxoammonium cation in the SOD-mimic activity of cyclic nitroxides. *J. Am. Chem. Soc.* **125**, 789–795 (2003).
- Stoyanovsky, D. A. & Cederbaum, A. I. Metabolism of carbon tetrachloride to trichloromethyl radical: An ESR and HPLC-EC study. *Chem. Res. Toxicol.* **12**, 730–736 (1999).
- Stoyanovsky, D. A., Melnikov, Z. & Cederbaum, A. I. ESR and HPLC-EC analysis of the interaction of hydroxyl radical with DMSO: rapid reduction and quantification of POBN and PBN nitroxides. *Anal. Chem.* **71**, 715–721 (1999).
- Baldwin, J. E. & Sklarz, B. Methylene nitrones, a new type of nitrones. *Chem. Commun. (London)* 373–374 (1968).
- Confalone, P. & Huie, E. The [3+2] Nitron-olefin cycloaddition reaction. Vol. 36 39 (John Wiley & Sons, Inc., 1988).

17. Dolbier, W. Jr., Purvis, G. III, Seabury, M., Wicks, G. & Burkholder, C. The regiochemistry and stereochemistry of 1,3-dipolar cycloadditions of 1-fluoro- and 1,1-difluoroallene. *Tetrahedron* **46**, 7991–8004 (1990).
18. Chalfont, G. R. & Perkins, M. J. A probe for homolytic reactions in solution. Part IV. The succinimidyl radical. *J. Chem. Soc. (B)*, 401–404 (1970).
19. Chalfont, G. R., Perkins, M. J. & Horsfield, A. A probe for homolytic reactions in solution. II. The polymerization of styrene. *J. Am. Chem. Soc.* **7142–7142** (1968).
20. Baldwin, J. E., Qureshi, A. K. & Sklarz, B. Aliphatic nitroso-compounds. Part I. Reactions with diazomethane. A new group of nitrones. *J. Chem. Soc. (C)*, 1073–1079 (1969).
21. Voinov, M. A. & Grigor'ev, I. A. Dipole-stabilized carbanion in the series of cyclic aldonitrones 3^* . The influence of the configuration of the nitronone group on H-D exchange of the methine hydrogen atom and metallation of aldonitrones. *Russ. Chem. Bull., Int. ed.* **51**, 297–305 (2002).
22. Kalyanaraman, B. Thiyl radicals in biological systems: significant or trivial? *Biochem. SOC. Symp.* **61**, 55–63 (1995).
23. Stoyanovsky, D. A., Maeda, A., Atkins, J. L. & Kagan, V. E. Assessments of thiyl radicals in biosystems: difficulties and new applications. *Anal. Chem.* **83**, 6432–6438 (2011).
24. Madej, E., Folkes, L. K., Wardman, P., Czapski, G. & Goldstein, S. Thiyl radicals react with nitric oxide to form S-nitrosothiols with rate constants near the diffusion-controlled limit. *Free Radic. Biol. Med.* **44**, 2013–2018 (2008).
25. Josephy, P., Rehorek, D. & Janzen, E. Electron spin resonance spin trapping of thiyl radicals from the decomposition of thionitrites. *Tetrahedron Lett.* **25**, 1685–1688 (1984).
26. Ross, D., Albano, E., Nilsson, U. & Moldeus, P. Thiyl radicals—formation during peroxidase-catalyzed metabolism of acetaminophen in the presence of thiols. *Biochem. Biophys. Res. Commun.* **125**, 109–115 (1984).
27. Ross, D., Norbeck, K. & Moldeus, P. The generation and subsequent fate of glutathionyl radicals in biological systems. *J. Biol. Chem.* **260**, 15028–15032 (1985).
28. Davies, M. J., Forni, L. G. & Shuter, S. L. Electron spin resonance and pulse radiolysis studies on the spin trapping of sulphur-centered radicals. *Chem. Biol. Interact.* **61**, 177–188 (1987).
29. Potapenko, D., Bagryanskaya, E., Tsentelovich, Y., Reznikov, V. & Khramstov, V. Reversible reactions of thiols and thiyl radicals with nitronone spin traps. *J. Phys. Chem. B* **108**, 9315–9324 (2004).
30. Sengupta, R., Billiar, T. R. & Stoyanovsky, D. A. Studies toward the analysis of S-nitrosoproteins. *Org. Biomol. Chem.* **7**, 232–234 (2009).
31. Stoyanovsky, D. A. *et al.* Detection and characterization of the electron paramagnetic resonance-silent glutathionyl-5,5-dimethyl-1-pyrroline N-oxide adduct derived from redox cycling of phenoxyl radicals in model systems and HL-60 cells. *Arch. Biochem. Biophys.* **330**, 3–11 (1996).
32. Hardy, M. *et al.* Detection, characterization, and decay kinetics of ROS and thiyl adducts of mito-DEPMPO spin trap. *Chem. Res. Toxicol.* **20**, 1053–1060 (2007).
33. Frejaville, C. *et al.* 5-(Diethoxyphosphoryl)-5-methyl-1-pyrroline N-oxide: a new efficient phosphorylated nitronone for the *in vitro* and *in vivo* spin trapping of oxygen-centered radicals. *J. Med. Chem.* **38**, 258–265 (1995).
34. Nilsen, N. & Braslau, R. Nitroxide Decomposition: Implications toward Nitroxide Design for Applications in Living Free-Radical Polymerization. *J. Polym. Sci. A* **44**, 697–717 (2006).
35. Jambhekar, S. S. & Breen, P. Cyclodextrins in pharmaceutical formulations II: solubilization, binding constant, and complexation efficiency. *Drug Discov. Today* **21**, 363–368 (2016).
36. Mao, J. *et al.* Host-guest complexes as water-soluble high-performance DNP polarizing agents. *J. Am. Chem. Soc.* **135**, 19275–19281 (2013).
37. Kotake, Y. & Janzen, E. G. Bimodal inclusion of nitroxide radicals by beta-cyclodextrin in water as detected by electron spin resonance resonance. *J. Am. Chem. Soc.* **110**, 3699–3701 (1988).
38. Lucarini, M., Luppi, B., Pedulli, G. F. & Roberts, B. P. Dynamic aspects of cyclodextrin host \pm guest inclusion as studied by an EPR spin-probe technique. *Chem. Eur. J.* **5**, 2048–2054 (1999).
39. Okazaki, M. & Kuwata, K. Molecular disposition of inclusion complexes of three aminoxyl radicals with beta-cyclodextrin in aqueous solution. *J. Phys. Chem.* **88**, 3163–3165 (1984).
40. Robert, L., VanEtten, R. L., Sebastian, J. F., Clowes, G. A. & Bender, M. L. Acceleration of phenyl ester cleavage by cyclodextrins. A model for enzymatic specificity. *J. Am. Chem. Soc.* **89**, 3242–3253 (1967).
41. Bardelang, D. *et al.* Alpha-phenyl-N-tert-butyl-nitronone-type derivatives bound to beta-cyclodextrins: syntheses, thermokinetics of self-inclusion and application to superoxide spin-trapping. *Chemistry* **13**, 9344–9354 (2007).
42. Bardelang, D. *et al.* Nitroxide bound beta-cyclodextrin: is there an inclusion complex? *J. Org. Chem.* **71**, 7657–7667 (2006).
43. Bardelang, D. *et al.* Inclusion complexes of EMPO derivatives with 2,6-di-O-methyl-beta-cyclodextrin: synthesis, NMR and EPR investigations for enhanced superoxide detection. *Org. Biomol. Chem.* **4**, 2874–2882 (2006).
44. Bardelang, D., Rockenbauer, A., Karoui, H., Finet, J. P. & Tordo, P. Inclusion complexes of PBN-type nitronone spin traps and their superoxide spin adducts with cyclodextrin derivatives: parallel determination of the association constants by NMR titrations and 2D-EPR simulations. *J. Phys. Chem. B* **109**, 10521–10530 (2005).
45. Beziere, N. *et al.* Metabolic stability of superoxide adducts derived from newly developed cyclic nitronone spin traps. *Free Radic. Biol. Med.* **67**, 150–158 (2014).
46. Karoui, H., Rockenbauer, A., Pietri, S. & Tordo, P. Spin trapping of superoxide in the presence of beta-cyclodextrins. *Chem. Commun. (Camb.)*, 3030–3031 (2002).
47. Harbour, J. R., Chow, V. & Bolton, J. R. An electron spin resonance study of the spin adducts of OH and HO₂ radicals with nitronones in the ultraviolet photolysis of aqueous hydrogen peroxide solutions. *Can. J. Chem.* **52**, 3549–3553 (1974).
48. Finkelstein, E., Rosen, G. M., Rauckman, E. J. & Paxton, J. Spin trapping of superoxide. *Mol. Pharmacol.* **16**, 676–685 (1979).
49. Rosen, G. M. & Turner, M. J., 3rd. Synthesis of spin traps specific for hydroxyl radical. *J. Med. Chem.* **31**, 428–432 (1988).
50. Allouch, A., Roubaud, V., Lauricella, R., Bouteiller, J. C. & Tuccio, B. Spin trapping of superoxide by diester-nitronones. *Org. Biomol. Chem.* **3**, 2458–2462 (2005).
51. Winterbourn, C. C. & Metodiewa, D. The reaction of superoxide with reduced glutathione. *Arch. Biochem. Biophys.* **314**, 284–290 (1994).
52. Dikalov, S., Kirilyuk, I. & Grigor'ev, I. Spin trapping of O-, C-, and S-centered radicals and peroxy-nitrite by 2H-imidazole-1-oxides. *Biochem. Biophys. Res. Commun.* **218**, 616–622 (1996).
53. Stoyanovsky, D. A., Goldman, R., Claycamp, H. G. & Kagan, V. E. Phenoxyl radical-induced thiol-dependent generation of reactive oxygen species: implications for benzene toxicity. *Arch. Biochem. Biophys.* **317**, 315–323 (1995).
54. Ashburn, S. P. & Coates, R. M. Generation and [3+2] Cycloaddition Reactions of Oxazoline N-Oxides. *J. Org. Chem.* **49**, 3127–3133 (1984).
55. Clancy, R., Cederbaum, A. I. & Stoyanovsky, D. A. Preparation and properties of S-nitroso-L-cysteine ethyl ester, an intracellular nitrosating agent. *J. Med. Chem.* **44**, 2035–2038 (2001).
56. Novakov, C. P., Feierman, D., Cederbaum, A. I. & Stoyanovsky, D. A. An ESR and HPLC-EC assay for the detection of alkyl radicals. *Chem. Res. Toxicol.* **14**, 1239–1246 (2001).

Acknowledgements

This work was supported by NIH Grants GM102146 (M.J.S.), GM044100 (T.R.B.), and U19AI068021-06 (D.A.S.). We thank Mr. Anastas Stoyanovsky (IBM Watson; Pittsburgh, PA, USA) for his critical reading of our paper.

Author Contributions

M.J.S. and D.A.S. planned the research work. D.A.S. synthesized EBN and performed EPR experiments. All the authors discussed the results and commented on the manuscript. D.A.S. wrote the manuscript.

Additional Information

Competing financial interests: The authors declare no competing financial interests.

How to cite this article: Scott, M. J. *et al.* *N-tert-butylmethanimine N-oxide* is an efficient spin-trapping probe for EPR analysis of glutathione thiyl radical. *Sci. Rep.* **6**, 38773; doi: 10.1038/srep38773 (2016).

Publisher's note: Springer Nature remains neutral with regard to jurisdictional claims in published maps and institutional affiliations.



This work is licensed under a Creative Commons Attribution 4.0 International License. The images or other third party material in this article are included in the article's Creative Commons license, unless indicated otherwise in the credit line; if the material is not included under the Creative Commons license, users will need to obtain permission from the license holder to reproduce the material. To view a copy of this license, visit <http://creativecommons.org/licenses/by/4.0/>

© The Author(s) 2016